Interactive 3D Human Heart Simulations on Segmented Human MRI Hearts

John P Berman[1], Abouzar Kaboudian[1], Ilija Uzelac[1], Shahriar Iravanian[2], Tinen Iles[3], Paul A Iaizzo[3], Hyunkyung Lim[4], Scott Smolka[4], James Glimm[4], Elizabeth M Cherry[5], Flavio H Fenton[1]

[1] School of Physics, Georgia Institute of Technology, Atlanta, GA, USA
[2] Division of Cardiology, Emory University, Atlanta, GA, USA
[3] Medical School, University of Minnesota, Minneapolis, MN, USA
[4] Stony Brook University, Stony Brook, NY
[5] School of Computational Science and Engineering, Georgia Institute of Technology, Atlanta, GA, USA

Abstract

Understanding cardiac arrhythmic mechanisms and developing new strategies to control and terminate them using computer simulations requires realistic physiological cell models with anatomically accurate heart structures. Furthermore, numerical simulations must be fast enough to study and validate model and structure parameters. Here, we present an interactive parallel approach for solving detailed cell dynamics in high-resolution human heart structures with a local PC's GPU. In vitro human heart MRI scans were manually segmented to produce 3D structures with anatomically realistic electrophysiology. The Abubu.js library was used to create an interactive code to solve the OVVR human ventricular cell model and the FDA extension of the model in the human MRI heart structures, allowing the simulation of reentrant waves and investigation of their dynamics in real time. Interactive simulations of a physiological cell model in a detailed anatomical human heart reveals propagation of waves through the fine structures of the trabeculae and pectinate muscle that can perpetuate arrhythmias, thereby giving new insights into effects that may need to be considered when planning ablation and other defibrillation methods.

1. Introduction

Simulations of complex models of cardiac cell electrophysiology in anatomically accurate 3D heart structures are useful for investigating among others, arrhythmia mechanisms [1, 2], drug cardiotoxicity [3] and personalized anti-arrhythmic therapies [4]. Although there are still problems with cardiac cell models failing to reproduce many tissue-level characteristics [5] and changes due to drug interactions [3], there are many current efforts aimed at sensitivity analysis [6], quantifying uncertainty [7], model calibration [8], model validation [9], verification [10], and studying variability [11] of electrophysiological models as well as to account for population diversity [12] and patient-specific [13] properties. Similarly, several efforts have been made to develop methods to solve these complex models in large domains using fast graphics processing units (GPUs) [14] so that simulations can be performed in real time and interactively on a single computer [15] with the goal of eventually being used in clinical situations. In this manuscript, we build upon the work of Bernabeu *et al.* [16], who performed some of the first high-resolution simulations of the Luo-Rudy 1 model in a highly discretized rabbit ventricular structure, by performing some of the first simulations on a whole high-resolution human heart with one of the most up-to-date human ventricular models, the O'Hara-Virág-Varró-Rudy (OVVR) [17], and a human atrial model used to fit clinical patient data [13].

2. Heart Preparation

The heart used in this study is one of hundreds that have been digitized with MRI by the Visible Heart Lab at the University of Minnesota[18]. All specimens were perfusion fixed with 10% formalin under pressure to preserve them in an end-diastolic state. For MRI scanning, the specimen was then filled and surrounded with an agarose gel to optimize the anatomic structures and minimize motion artifacts during scanning. The stack of MRI images (see examples in Figure 1) consist of 280×251 pixels in width and $\times 450$ in pixels in height. The images were post-processed using ImageJ. First, all fatty and connective tissue was deleted manually frame by frame, then all pixels were normalized to have the same contrast to clearly identify cardiac tissue. The resolution of the MRI allows for many details in the atria, including large sections of pectinate muscle on the interior surface of both atria, par-

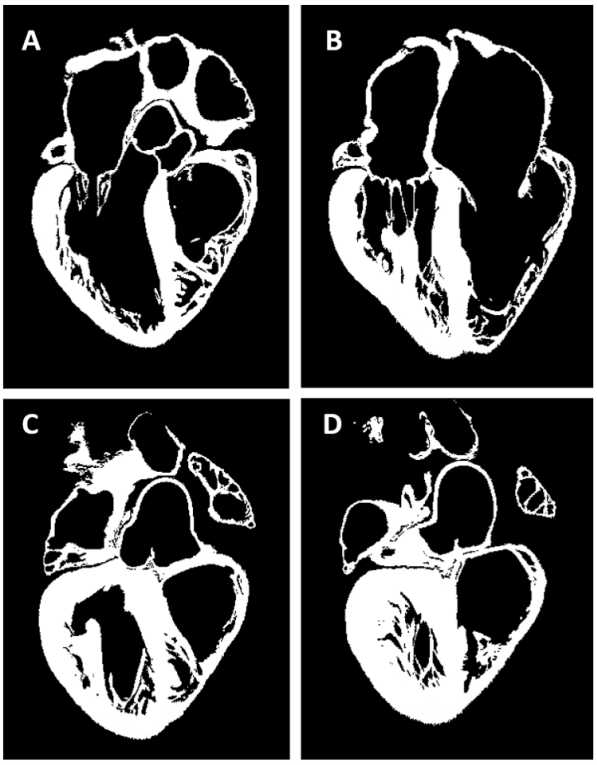

Figure 1. Examples of 2D MRI sections from a human heart (posterior views, A-D) after homogenization of all pixel intensities and deletion of fatty and connective tissue. Views show right and left atria and right and left ventricles in addition to many details, such as pectinate muscles in the atria, especially within the atrial appendages (C-D), and trabecule connecting tissue all along the right and left ventricles, as well as valves and tendons.

ticularly within the atrial appendages, as shown in Figure 1C-D. Similarly, large regions of well-resolved trabeculae are observed along the endocardium of the right and left ventricles (Figure 1A-D). Similarly, tendons and valves are well resolved in this structure, as shown in Fig. 1B. The 3D structure can be reconstructed directly from the post-processed MRI data using a uniform mesh, as shown in Figure 2, which display different clipped views of the full 3D heart to display the heart's interior.

3. Numerical Methods

The data points from the uniform 3D heart mesh are imported as an unstructured mesh for fast processing and simulation of the coupled reaction-diffusion equations of the cell and tissue electrophysiology using finite differences. The spatial resolution of the mesh is $\delta x = 0.02\text{cm}$, so that the heart size overall is about $5.6\text{cm} \times 5\text{cm} \times 9.6\text{cm}$ in size, corresponding to a small individual. The numeri-

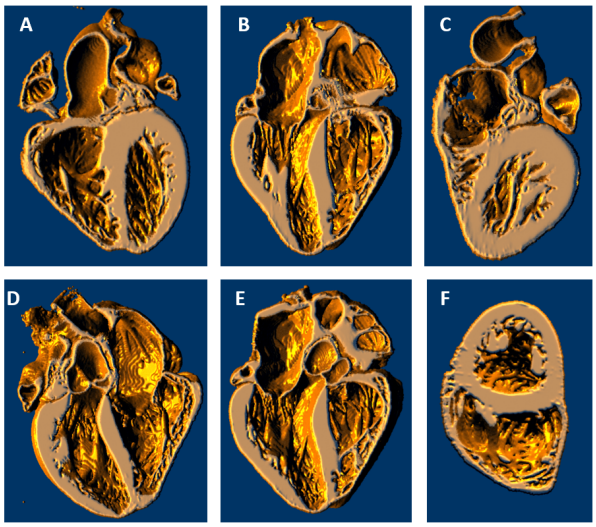

Figure 2. 3D reconstruction of the human heart from the MRI scan data. The clipped views illustrate the different thicknesses of the atria, right ventricle, septum and left ventricle.

cal time step is $\delta t = .01ms$ and the diffusion coefficient is $D = 0.001\text{cm}^2/\text{ms}$. The integration of the ventricular (OVVR < 41 variables per cell) and atrial (4 variables per cell) models in the 3D heart domain is performed using our custom WebGL library *Abubu.js* that runs on the GPU of the device where the program is launched [15]. This software allows interactive simulations and visualization of electrical waves in the 3D human heart on any device *(desktop computers, laptops, tablets,* and even *smart phones* with enough memory*)*, independent of operating system *(unix/Linux, Widows, MacOS)*, without the need for compiling or installing any plugins.

Fiber orientation is added following a Laplace–Dirichlet Rule-Based (LDRB) algorithm to generate the fiber orientations inside the ventricles. The detailed algorithm [19] solves Laplace's equations with the Dirichlet boundary conditions assigned by the apex, base and epicardial surfaces of the ventricles and the endocardial surfaces of the left and right ventricles (Figure 3). The potential gradients of the solutions are smooth and used for constructing the fiber directions wrapping around the internal structures of the heart, such as blood vessels and trabeculae. Furthermore, a bi-directional spherical linear interpolation achieves continuous fiber orientation within the myocardium.

For excitations in the tissue, we perform a distance search from the mouse click to the surface of the tissue so that voltage activations can be created each time the mouse is clicked, at the surface nearest to the click. In this way, waves can be initiated anywhere in the heart (both atria and ventricles); in particular, reentrant spiral waves can be in-

duced using the S1-S2 protocol[20]. In addition, the Purkinje activation sequence as identified by Durrer *et al.* [21] can be initiated.

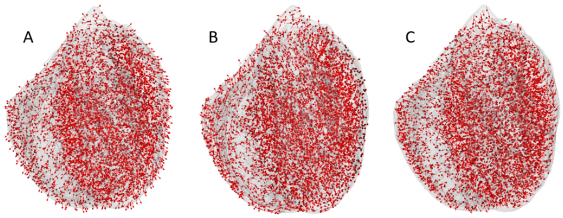

Figure 3. 3D reconstruction of ventricular fibers. Image shows views of fibers that are (A) transverse, (B) longitudinal and (C) normal to the sheets.

4. Results

Using the WebGL software [22, 23], we were able to perform fast real-time simulations in the separated and combined structure. Figure 4 shows disorganized activity corresponding to a reentrant arrhythmia in the atrial structure. A wavefront (green) can be seen crossing Bachmann's bundle (A) and propagating within the right atrium (B-C). Electrical activity is also visible on the endocardial surfaces, including the pectinate muscles.

Figure 5 displays a reentrant wave in the ventricular structure. The cut-away views show a wave propagating in the left ventricle and septum toward the apex; activity can also be seen on the trabeculated endocardial surface of the right ventricle.

Simulations within the full heart are shown in Figure 6, with fibrillation present in all chambers.

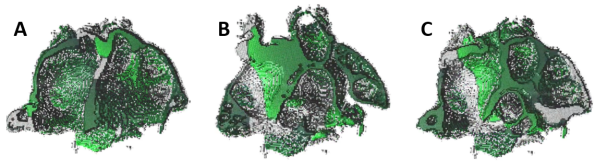

Figure 4. Simulation of reentrant arrhythmias in the atria alone. (A-C) Three clipped views of the the 3D atria are shown at one moment in time. Green indicates depolarized tissue and gray represents tissue at rest (polarized tissue).

5. Conclusions and Future work

We have shown the power and flexibility of our WebGL simulation and visualization software using a human heart structure. Both the atria alone and ventricles alone can be used during simulations, or propagation can be simulated within the entire heart. During arrhythmic behavior, we observed propagation within the pectinate muscles and trabeculae that may play a role during reentrant arrhythmias.

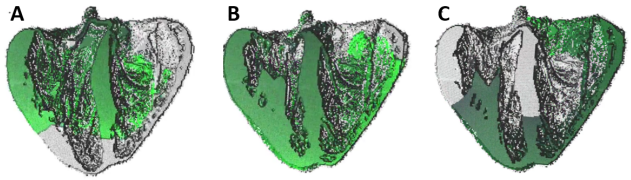

Figure 5. Simulation of reentrant arrhythmias in the ventricles alone. (A-C) Three clipped views of the the 3D ventricles at one moment in time. Colors are as in Figure 4.

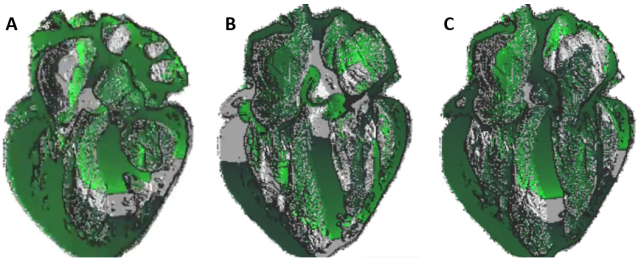

Figure 6. Simulations of reentrant arrhythmias in the whole 3D heart. (A-C) Three clipped views of the the 3D heart at one moment in time during ventricular and atria fibrillation. Green indicates depolarized tissue and gray represents tissue at rest (polarized tissue).

As next steps, we intend to continue studying the role of geometrical features on reentrant wave patterns and dynamics. We expect that inclusion of some of these anatomical details may be needed to plan appropriate personalized therapy for arrhythmias via ablation or other techniques. Due to its efficiency, flexibility, and interactivity, our near-real-time simulation and visualization environment has the potential to contribute to efforts to develop such individualized treatments in the clinic.

Acknowledgments

This study was supported in part by the National Science Foundation grants NSF-FDA-2037894 (FHF,AK), CMMI-2011280 (EMC), CNS-1446675, CMMI-1762553 (FHF) and CPS-1446832 (SAS), and by the National Institutes of Health grant 1R01HL143450-01 (EMC and FHF).

References

[1] Aslanidi OV, Colman MA, Stott J, Dobrzynski H, Boyett MR, Holden AV, Zhang H. 3d virtual human atria: A computational platform for studying clinical atrial fibrilla-

tion. Progress in biophysics and molecular biology 2011; 107(1):156–168.

[2] Cherry EM, Fenton FH. Effects of boundaries and geometry on the spatial distribution of action potential duration in cardiac tissue. Journal of Theoretical Biology 2011; 285(1):164–176.

[3] Uzelac I, Kaboudian A, Iravanian S, Siles-Paredes JG, Gumbart JC, Ashikaga H, Bhatia N, Gilmour Jr RF, Cherry EM, Fenton FH. Quantifying arrhythmic long qt effects of hydroxychloroquine and azithromycin with whole-heart optical mapping and simulations. Heart Rhythm O2 2021;.

[4] Prakosa A, Arevalo HJ, Deng D, Boyle PM, Nikolov PP, Ashikaga H, Blauer JJ, Ghafoori E, Park CJ, Blake RC, et al. Personalized virtual-heart technology for guiding the ablation of infarct-related ventricular tachycardia. Nature Biomedical Engineering 2018;2(10):732–740.

[5] Uzelac I, Ji YC, Hornung D, Schröder-Scheteling J, Luther S, Gray RA, Cherry EM, Fenton FH. Simultaneous quantification of spatially discordant alternans in voltage and intracellular calcium in langendorff-perfused rabbit hearts and inconsistencies with models of cardiac action potentials and ca transients. Frontiers in Physiology 2017;8:819.

[6] Pathmanathan P, Cordeiro JM, Gray RA. Comprehensive uncertainty quantification and sensitivity analysis for cardiac action potential models. Frontiers in Physiology 2019; 10:721.

[7] Pathmanathan P, Galappaththige SK, Cordeiro JM, Kaboudian A, Fenton FH, Gray RA. Data-driven uncertainty quantification for cardiac electrophysiological models: impact of physiological variability on action potential and spiral wave dynamics. Frontiers in Physiology 2020;11:1463.

[8] Whittaker DG, Clerx M, Lei CL, Christini DJ, Mirams GR. Calibration of ionic and cellular cardiac electrophysiology models. Wiley Interdisciplinary Reviews Systems Biology and Medicine 2020;12(4):e1482.

[9] Barone A, Gizzi A, Fenton F, Filippi S, Veneziani A. Experimental validation of a variational data assimilation procedure for estimating space-dependent cardiac conductivities. Computer Methods in Applied Mechanics and Engineering 2020;358:112615.

[10] Pathmanathan P, Gray RA. Verification of computational models of cardiac electro-physiology. International Journal for Numerical Methods in Biomedical Engineering 2014; 30(5):525–544.

[11] Muszkiewicz A, Britton OJ, Gemmell P, Passini E, Sánchez C, Zhou X, Carusi A, Quinn TA, Burrage K, Bueno-Orovio A, et al. Variability in cardiac electrophysiology: using experimentally-calibrated populations of models to move beyond the single virtual physiological human paradigm. Progress in Biophysics and Molecular Biology 2016;120(1-3):115–127.

[12] Sarkar AX, Christini DJ, Sobie EA. Exploiting mathematical models to illuminate electrophysiological variability between individuals. The Journal of Physiology 2012; 590(11):2555–2567.

[13] Lombardo DM, Fenton FH, Narayan SM, Rappel WJ. Comparison of detailed and simplified models of human atrial myocytes to recapitulate patient specific properties. PLoS Computational Biology 2016;12(8):e1005060.

[14] Sachetto Oliveira R, Martins Rocha B, Burgarelli D, Meira Jr W, Constantinides C, Weber dos Santos R. Performance evaluation of gpu parallelization, space-time adaptive algorithms, and their combination for simulating cardiac electrophysiology. International Journal for Numerical Methods in Biomedical Engineering 2018;34(2):e2913.

[15] Kaboudian A, Cherry EM, Fenton FH. Real-time interactive simulations of large-scale systems on personal computers and cell phones: Toward patient-specific heart modeling and other applications. Science Advances 2019; 5(3):eaav6019.

[16] Bernabeu M, Bishop M, Pitt-Francis J, Gavaghan D, Grau V, Rodriguez B. High performance computer simulations for the study of biological function in 3d heart models incorporating fibre orientation and realistic geometry at paracellular resolution. In 2008 Computers in Cardiology. IEEE, 2008; 721–724.

[17] O'Hara T, Virág L, Varró A, Rudy Y. Simulation of the undiseased human cardiac ventricular action potential: model formulation and experimental validation. PLoS Computational Biology 2011;7(5):e1002061.

[18] Iaizzo PA. The visible heart® project and free-access website 'atlas of human cardiac anatomy'. EP Europace 2016; 18(suppl_4):iv163–iv172.

[19] Bayer JD, Blake RC, Plank G, Trayanova NA. A novel rule-based algorithm for assigning myocardial fiber orientation to computational heart models. Annals of biomedical engineering 2012;40(10):2243–2254.

[20] Winfree AT. Electrical instability in cardiac muscle: phase singularities and rotors. Journal of theoretical Biology 1989;138(3):353–405.

[21] Durrer D, Van Dam RT, Freud G, Janse M, Meijler F, Arzbaecher R. Total excitation of the isolated human heart. Circulation 1970;41(6):899–912.

[22] Kaboudian A, Velasco-Perez HA, Iravanian S, Shiferaw Y, Cherry EM, Fenton FH. A comprehensive comparison of gpu implementations of cardiac electrophysiology models. In From Reactive Systems to Cyber-Physical Systems. Springer, 2019; 9–34.

[23] Kaboudian A, Cherry EM, Fenton FH. Large-scale interactive numerical experiments of chaos, solitons and fractals in real time via gpu in a web browser. Chaos Solitons Fractals 2019;121:6–29.

Address for correspondence:

Flavio H. Fenton
School of Physics
Georgia Institute of Technology
Atlanta, GA, USA
flavio.fenton@gatech.edu